Nuclear Engineering and Technology xxx (2016) 1–17

Available online at ScienceDirect

Nuclear Engineering and Technology

journal homepage: www.elsevier.com/locate/net

Original Article

Comparative Experiments to Assess the Effects of Accumulator Nitrogen Injection on Passive Core Cooling During Small Break LOCA

Li Yuquan[*], *Hao Botao*, *Zhong Jia*, *and Wang Nan*

State Nuclear Power Technology R&D Center, South Park, Beijing Future Science & Technology City, Beijing 102209, China

ARTICLE INFO

Article history:
Received 9 January 2016
Received in revised form
11 April 2016
Accepted 30 June 2016
Available online xxx

Keywords:
Accumulator
Nitrogen gas
Core cooling
Passive safety
Small break

ABSTRACT

The accumulator is a passive safety injection device for emergency core cooling systems. As an important safety feature for providing a high-speed injection flow to the core by compressed nitrogen gas pressure during a loss-of-coolant accident (LOCA), the accumulator injects its precharged nitrogen into the system after its coolant has been emptied. Attention has been drawn to the possible negative effects caused by such a nitrogen injection in passive safety nuclear power plants. Although some experimental work on the nitrogen injection has been done, there have been no comparative tests in which the effects on the system responses and the core safety have been clearly assessed. In this study, a new thermal hydraulic integral test facility—the advanced core-cooling mechanism experiment (ACME)—was designed and constructed to support the CAP1400 safety review. The ACME test facility was used to study the nitrogen injection effects on the system responses to the small break loss-of-coolant accident LOCA (SBLOCA) transient. Two comparison test groups—a 2-inch cold leg break and a double-ended direct-vessel-injection (DEDVI) line break—were conducted. Each group consists of a nitrogen injection test and a nitrogen isolation comparison test with the same break conditions. To assess the nitrogen injection effects, the experimental data that are representative of the system responses and the core safety were compared and analyzed. The results of the comparison show that the effects of nitrogen injection on system responses and core safety are significantly different between the 2-inch and DEDVI breaks. The mechanisms of the different effects on the transient were also investigated. The amount of nitrogen injected, along with its heat absorption, was likewise evaluated in order to assess its effect on the system depressurization process. The results of the comparison and analyses in this study are important for recognizing and understanding the potential negative effects on the passive core cooling performance caused by nitrogen injection during the SBLOCA transient.

* *Corresponding author.*
E-mail address: liyuquan@snptc.com.cn (L. Yuquan).

http://dx.doi.org/10.1016/j.net.2016.06.014

Please cite this article in press as: L. Yuquan et al., Comparative Experiments to Assess the Effects of Accumulator Nitrogen Injection on Passive Core Cooling During Small Break LOCA, Nuclear Engineering and Technology (2016), http://dx.doi.org/10.1016/j.net.2016.06.014

1. Introduction

The accumulator (ACC) is a pressurized safety injection tank. It is one of the main components of a passive safety injection system in a nuclear power plant [1]. Under normal operations, the ACC contains both the cold coolant and the precharged nitrogen gas (N_2) in a single tank. In the event of a loss-of-coolant accident (LOCA) and when the reactor coolant system (RCS) pressure falls below the precharged nitrogen pressure, the coolant discharges from the ACC at high speed into the core.

In Generation III+ reactors, the passive safety pressurized water reactors (PWRs), including AP600 [2], AP1000 [3], and CAP1400 [4], rely only on natural forces or processes, such as gravity and compressed gas pressure, to provide the safety injection and to perform the function of the emergency core cooling system (ECCS). As shown in Fig. 1, these reactors have a two-loop RCS configuration and are equipped with a passive safety core cooling system (PXS). In the PXS, the spherical ACCs are connected to the reactor pressure vessel (RPV) through the direct vessel injection (DVI) lines. When the ACC is empty, the RCS is depressurized and N_2 is expanded. The N_2 in the tank is then injected into the system. The effects of this N_2 injection on the passive core cooling process under a small break LOCA (SBLOCA) scenario is a technical concern. Potentially, it could have negative effects, such as slowing down the depressurization and stopping the ECCS injection, leading to the failure of core cooling [5]. The SBLOCA phenomena identification and ranking table (PIRT) of the AP600 reactor once ranked the ACC noncondensable gas entrainment as "plausible (P)" [6]. This ranking indicates that the effects of N_2 injection on the passive core cooling system performance need to be evaluated.

In order to support the development and safety review of the AP600/1000 reactor, three integral test facilities have been developed. They are a full-height, full-pressure, and 1/30.5 volume scale integral test facility named the Rig of safety assessment (ROSA) of Japan Atomic Energy Research Institute (JAERI, Tokai-mura, Naka-gun, Ibaraki-ken 319-11, Japan) [7], a full-height, full-pressure, 1/395 volume scale test facility named the SPES-2 in Italy [8], and a 1/4 height scale and reduced-pressure integral test facility named the Advanced Plant Experimental (APEX) test facility in the United States [6]. By analyzing the experimental data from these three integral tests, the potential effects of ACC N_2 injection on the passive core cooling performance have been studied.

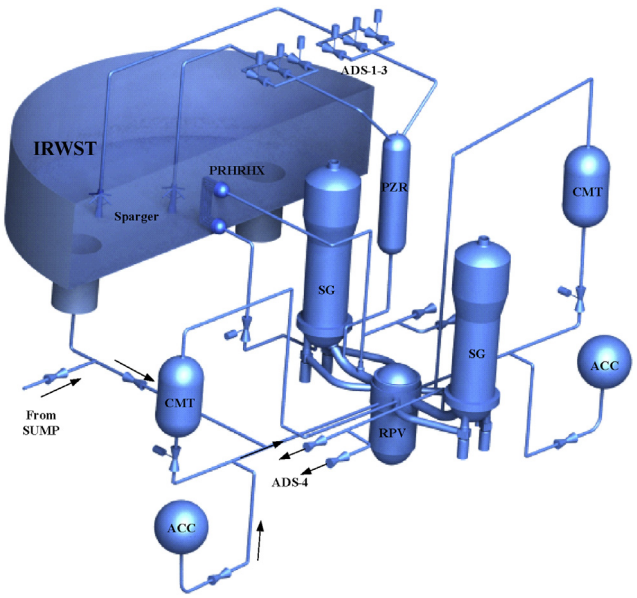

Fig. 1 – Schematic diagram of the RCS and PXS in a passive safety PWRs. PWR, pressurized water reactor; PXS, passive safety core cooling system; RCS, reactor coolant system.

The ROSA integral test results show that the impact of this noncondensable gas injection on the core cooling performance is insignificant. However, an analysis of the experimental data shows that when nitrogen enters the core makeup tank (CMT), it can suppress the steam condensation in the CMT, but improve the drainage of the CMT [5,7]. Further analysis of the SPES-2 SBLOCA experimental data shows that the injected N_2 can enter the CMT. Additionally, N_2 potentially reduces the effectiveness of the passive residual heat removal (PRHR) performance. This is because when the ACC N_2 injection starts, the PRHR heat removal role is already coming to an end [9]. Moreover, the N_2 transport in the system has been investigated experimentally at the APEX test facility [10]. The test data show that nitrogen can enter into the CMT, PRHR, RPV, and in-containment refueling water storage tank (IRWST); however, no quantitative information has been made available [11].

Although some experimental works have been carried out, the effects of N_2 injection on the core safety and the system responses and the control mechanisms still need to be studied. First, in addition to the investigation of how N_2 affects the local processes, such as CMT drainage and PRHR circulation, the effects of N_2 injection on system responses and core safety also need to be studied. This is because whether N_2 injection can change the core safety-related parameters, such as system pressure, cooling flow rate, and core level, is still unclear. Second, there are no comparative tests to show the effects of N_2 injection. As compared to the earlier analyses of the test data from the three facilities, an analysis of the comparative test results is a more convincing and effective approach to show the effects of N_2.

One comparative test group consists of two SBLOCA tests. All the initial and boundary conditions of the two tests—such as the break, the initial steady-state parameters, the decay power, and the safety system alignment—are the same. There is only one difference between the two tests. In one test, the ACC is allowed to inject its nitrogen into the system when it is empty, just like the process in the prototypes. In the other test, the ACC is isolated immediately once it is empty. Based on the experimental data from these two SBLOCA tests, system responses and important parameters were compared. From the comparison, the effects of N_2 injection on system performance and SBLOCA transient were determined. If such a comparative test group can be conducted in an integral test facility, this is a good way to study the effects of ACC N_2 injections. Unfortunately, such a comparative test cannot be conducted in the three integral test facilities mentioned earlier because the ACC and its injection line configuration in these test facilities are the same as that in the prototype.

Please cite this article in press as: L. Yuquan et al., Comparative Experiments to Assess the Effects of Accumulator Nitrogen Injection on Passive Core Cooling During Small Break LOCA, Nuclear Engineering and Technology (2016), http://dx.doi.org/10.1016/j.net.2016.06.014

In this study, the effects of N_2 injection were investigated using a new integral test facility, called the ACME (advanced core-cooling mechanism experiment). The ACME test facility was designed and built to support the CAP1400 reactor licensing and also to investigate the thermal hydraulic behaviors during the SBLOCA transient in a passive safety PWR. By adding an isolation valve on each ACC injection line in the ACME, N_2 injection comparative tests can be performed. There are two typical SBLOCA conditions that are essential in the AP600/1000 test programs: the 2-inch cold leg and the double-ended DVI (DEDVI) breaks. These two conditions have been included in the comparative test groups. By analyzing the results of the comparative tests, the effects of ACC N_2 injection on system responses, core safety, and important thermal hydraulic behaviors were investigated. The effects of N_2 on system responses and core safety were also analyzed. Finally, the amount of N_2 injected into the system and its effects on the system depressurization were also evaluated.

2. Possible effects of ACC nitrogen injection

2.1. ACC injection event in SBLOCA chronology

As shown in Fig. 1, there are three water sources for the safety injection when an SBLOCA happens. The first is from the CMT, which delivers the coolant to the system at any system pressure because it is connected to the RCS through the pressure balance line (PBL). The second is the ACC, which starts to inject its coolant into the system by the precharged N_2 when the system pressure falls below the charge pressure of 4.83 MPa. The third is from the IRWST, which starts the long-term gravity injection by its water head when the system is thoroughly depressurized, to near the containment atmosphere pressure. Among these three water injection sources, the ACC injection normally has the highest flow rate as its pressurized N_2 provides sufficient injection driving force. The main design parameters for the ACC in the AP600, AP1000, CAP1400, and the ACME test facility are listed in Table 1. It can be seen that nitrogen pressure and gas phase volume fraction are the same. Furthermore, the ACC volume in CAP1400 is 38% larger than those in AP600 and AP1000, whose ACC volumes are the same. The bigger ACC volume in CAP1400 approximately corresponds to the larger core power from the AP1000.

Fig. 2 shows the SBLOCA chronology of the passive safety PWRs and the general operation of the PXS. The SBLOCA transient is typically divided into five phases [12]: initial blowdown (1st phase), passive heat removal (2nd phase), ADS-1-3 depressurization (3rd phase), ADS-4 depressurization (4th phase), and injection from the IRWST and the sump (5th phase).

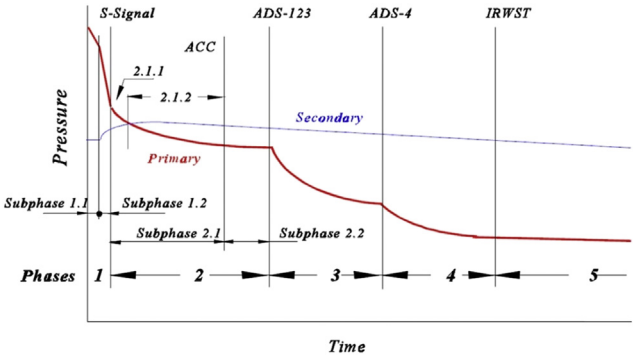

Fig. 2 – The phase sequence of SBLOCA transient. SBLOCA, small break loss-of-coolant accident.

The first phase is the initial blowdown phase, in which the system is depressurized from 15.5 MPa because of the mass and energy discharge through the break. The S-Signal occurs at 12.8 MPa, which results in an opening of the isolation valves of the CMT and passive residue heat removal (PRHR) heat exchanger (HX). Once the CMT and PRHR are actuated, the system moves into the second phase, in which the two closed natural circulation loops run for the core decay heat removal. The CMT then drains its water, which eventually reaches the "Low" level, and the ADS-1 is actuated. Normally, the ACC injection starts after the first two phases.

The third phase is the ADS-1-3 depressurization phase, which begins once ADS-1 is actuated and ends when ADS-4 is actuated. Once ADS-1 is actuated, ADS-2 and ADS-3 are subsequently actuated in sequence by a preset timer. This is to provide a gradual increase in the vent area for the primary system to depressurize. During this phase, the injection of the ACC begins when the system pressure falls below the ACC nitrogen pressure of 4.83 MPa. Because of the high injection flow rate of the ACC, the CMT injection is inhibited temporarily and then restarts after the emptying of ACCs. When the CMT level drops to the "Low–Low" set point, ADS-4 is actuated after a preset time delay. Therefore, the ACC coolant injection is normally completed within the ADS-1-3 depressurization phase, because the CMT drain is inhibited by the ACC injection, and hence this prevents the actuation of ADS-4. However, in a DEDVI break case, the emptying of the ACC is delayed, and so it comes later than the actuation of ADS-4, because ADS-4 is actuated by the CMT on the break side, which empties immediately when the break occurs.

The fourth phase is the ADS-4 depressurization phase. The opening of the ADS-4 increases the system depressurization rate. Normally during this phase, the ACC is already empty, but the N_2 remains in the ACC, and can still be injected into the system as the system is being depressurized by ADS-4. Once the system pressure falls below the water head in the IRWST, the coolant starts to be injected into the system by gravity. Earlier studies show that the minimum core level occurs during this phase [5,9–11,13]. Prior to the onset of

Table 1 – Main design parameters of ACC in AP600, AP1000, CAP1400, and ACME.

Main design parameter	AP600	AP1000	CAP1400	ACME
ACC volume (m^3)	56.63	56.63	78.26	0.836
Nitrogen pressure (MPa)	4.83	4.83	4.83	4.83
ACC gas phase volume fraction	0.85	0.85	0.85	0.85

ACC, accumulator; ACME, advanced core-cooling mechanism experiment.

Please cite this article in press as: L. Yuquan et al., Comparative Experiments to Assess the Effects of Accumulator Nitrogen Injection on Passive Core Cooling During Small Break LOCA, Nuclear Engineering and Technology (2016), http://dx.doi.org/10.1016/j.net.2016.06.014

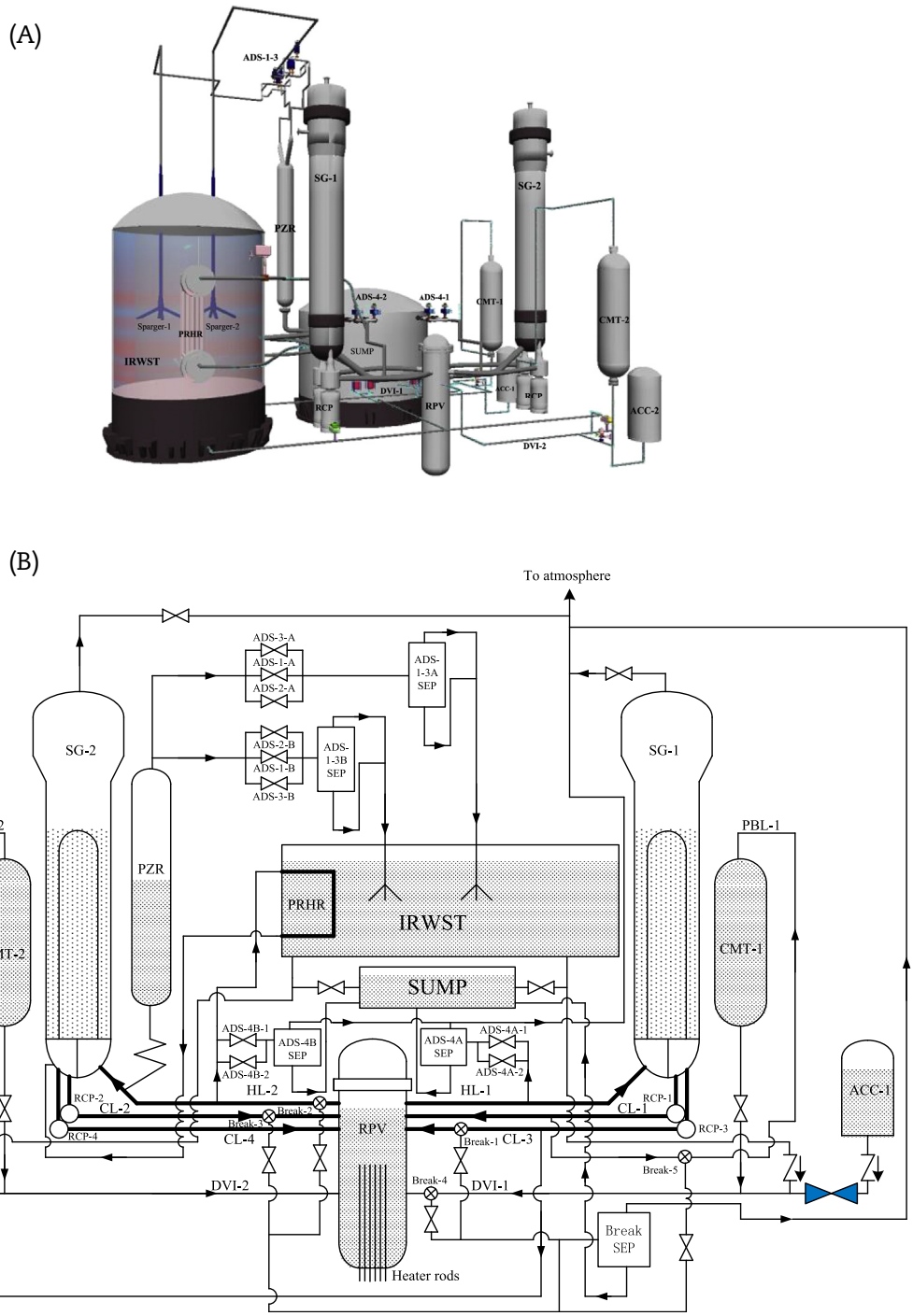

Fig. 3 – A 3D view and the schematic flow diagram of ACME test facility. (A) 3D view of ACME test facility. (B) Schematic flow diagram of ACME test facility. ACME, advanced core-cooling mechanism experiment; 3D, three dimensional.

IRWST injection, the core inventory is largely deprived by the ADS-4 discharge [14–18]. Any possible effect of ACC N_2 injection on core level should be a concern, because the minimum core level is critical for core safety during the SBLOCA transient.

The fifth phase is the IRWST and SUMP injection phase. During this phase, core cooling is maintained by the IRWST gravity injection and then by the SUMP recirculation. During long-term cooling, the ACC no longer discharges its N_2 into the system after the ACC is depressurized to the system pressure. Additionally, N_2 gradually leaves the system through the ADS venting paths and break. So, during this last long-term phase, N_2 does not cause a concern.

2.2. *Possible effects of ACC nitrogen injection*

As shown in Fig. 1, because the three water tanks are connected through one common DVI line, there could be

Please cite this article in press as: L. Yuquan et al., Comparative Experiments to Assess the Effects of Accumulator Nitrogen Injection on Passive Core Cooling During Small Break LOCA, Nuclear Engineering and Technology (2016), http://dx.doi.org/10.1016/j.net.2016.06.014

interactions among the three injections. Furthermore, because of the increase in the back pressure of the DVI line during ACC injection, the flow from the CMT may be reduced or even temporarily stopped [19]. Accordingly, N_2 injection can also suppress the drainage of the CMT and even the drainage of the IRWST after the ACC becomes empty. This is a negative effect as it decreases the injection flow rate.

As the noncondensable gas injection can cause a possible pressurization effect on the system, ADS depressurization can slow down because of the N_2 injection. This has a negative effect on core cooling because a timely onset of IRWST is critical for increasing the core level from the minimum level, and this rise in level requires a fast depressurization.

The noncondensable gas then mixes with the steam and could potentially reduce the effectiveness of the heat transfer by steam condensation, especially for the PRHR decay heat removal process [5]. However, the role of PRHR in cooling mainly takes place during the passive heat removal phase, and has already come to the end when the ACC is empty. Hence, this effect is insignificant to core cooling, even though it is negative. Additionally, the expansion of N_2 absorbs the heat. So, it is a source of cooling, which is positive for the system's depressurization and cooling.

Therefore, the possible effects of the ACC N_2 injection on the system can be summarized, as follows: (1) the ACC N_2 injection can suppress the drainage of the CMT and even the drainage of the IRWST, which can cause the injection flow rate to decrease, thereby lowering the core inventory; (2) the noncondensable gas can slow down the system depressurization, which can delay the IRWST injection startup, thereby lowering the minimum core level; and (3) the noncondensable gas can reduce the steam condensation heat transfer efficiency in the system, but the expansion of the gas can absorb the system heat. Hence, the consequential effects are still unknown.

3. The ACME test facility

As shown in Fig. 3A, the ACME test facility is a scaled-down model of the CAP1400 reactor, which is 1/3 height, 1/94 volume, and 1/54 power scale of the prototype [20]. The CAP1400 RCS and PXS layouts, including the interconnecting pipe routings and spatial geometry, have been simulated in the model as accurately as possible. The schematic flow of the ACME system is shown in Fig. 3B, the RCS and PXS of which are the same as those in the prototype.

As shown in Fig. 3A, although the shape of the ACC in the ACME test facility is different from that in the prototype, its elevation, volume, and inventory have been properly scaled. More importantly, in order to conduct the N_2 injection comparative tests, one isolation valve has been installed on each ACC injection line, as highlighted in Fig. 3B. These valves are not in the prototype. The ACC injection isolation valve is a quick shut valve, which automatically shuts when the liquid level in the ACC drops to nearly zero. In the ACME test facility, as the valve requires a certain time to be fully shut and there is uncertainty in the level detector, a 5-mm liquid depth has been set in the facility control logic to close the valve. In this study, the simulated breaks are on the CL-3 (Break-1) and DVI-1 (Break-4).

As shown in Fig. 3B, five liquid–steam separators are connected to the break, two trains of the ADS-1-3, and two sets of the ADS-4. Using the specially designed Break and ADS Measurement System (BAMS), the liquid and steam flow rates from the break and the ADS were measured individually.

Based on a pressure scheme study, the ACME's maximum operation pressure was determined to be 9.2 MPa [21]. The ACC injection and nitrogen discharge processes can be simulated under the prototypic pressure during the SBLOCA transient. Table 2 contains the main design parameters of the ACME test facility and their respective scale ratios.

As it is a scaled-down test facility, in order to ensure that ACME is able to simulate the important thermal hydraulic

Table 2 – Main design parameters and their scale ratios in the ACME test facility.

ACME design parameter	Scale ratio
Height	1:3
Fluid velocity	1:1.732
Flow area	1:31
Power	1:54
Time	1:1.732
RCS	
Loop configuration	2-loop
Core power (MW)	4.2
Core flow area scale	1:31
Design pressure (MPa)	10
Maximum Operation pressure (MPa)	9.2
Maximum coolant temperature (°C)	305
RCP	4 canned pumps
Inner diameter scale of CL and HL	1:4.9
Number of fuel rod simulators	180
Outer diameter of rods (mm)	11
Axial power distribution	Chopped cosine
Maximum cladding temperature (°C)	700
Number of U-tubes per SG	376
Total U-tube flow area scale	1:31
Secondary side	
Design pressure (MPa)	8.27
Normal operation pressure (MPa)	6.3–7.0
PORV pressure set point (MPa)	7.9
PXS	
CMT/ACC elevation scale	1:3
CMT internal height	1:3
CMT internal diameter	1:5.6
IRWST liquid level scale	1:3/1:1
CMT/ACC/IRWST volume scale	1:94
ACC nitrogen pressure (MPa)	4.83
CMT injection line resistance scale	1:1
ACC/IRWST injection line resistance scale	3:1
ADS-1-4	
Flow area scale	1:54
Scale factor of line resistance	3:1
DVI lines	
Trains	2 trains
Inner diameter scale	1:5.4

ACC, accumulator; ACME, advanced core-cooling mechanism experiment; CMT, core makeup tank; DVI, direct vessel injection; IRWST, in-containment refueling water storage tank; PXS, passive safety core cooling system; PORV, pressure operated relief valve; RCP, reactor coolant pump; RCS, reactor coolant system.

Please cite this article in press as: L. Yuquan et al., Comparative Experiments to Assess the Effects of Accumulator Nitrogen Injection on Passive Core Cooling During Small Break LOCA, Nuclear Engineering and Technology (2016), http://dx.doi.org/10.1016/j.net.2016.06.014

phenomena in the SBLOCA transient, as identified by the PIRT [22], ACME was designed using the detailed scaling analysis based on H2TS scaling methodology [23]. This analysis had also been used in scaling the APEX facility [6]. The effect of the reduced height on the test was evaluated mainly through the scaling distortion calculation, and the results show that the distortions are acceptable [24]. Moreover, ACC injection is driven by compressed gas, and hence the scale height effect has little impact on ACC injection simulation.

As an integral test facility, ACME has a total of > 1,100 instruments for the thermal hydraulic study and code benchmark. All instruments have been calibrated according to the quality assurance (QA) program. The thermocouple (TE) was used to measure the temperature of the fluid or the structures in various components. Furthermore, custom-made multipoint TE rods were installed in the RPV, CMTs, and IRWST for thermal stratification detection. Both narrow-range (NR) and wide-range (WR) pressure transducers (PTs) were used to measure the system pressure. The water level (LDP) was measured using differential pressure transducers, which gives the uncompensated level data. By adjusting these data according to the fluid temperature, the adjusted data are the compensated level data. As the core mixture level (LM) is a critical parameter, it has been measured using a guided wave radar. The liquid flow rates in the pipes and liquid lines were measured using the bar flow meters (FE), whereas the vapor flow rates in the steam lines were measured using the vortex flow meters (FV). The combination errors were analyzed, and the expanded uncertainty of every instrument was calculated [25]. Table 3 shows the instruments used in the ACME test facility and their respective errors.

The data acquisition system (DAS) of the ACME test facility is part of the Distributed Control System (DCS), which was used to perform data collection, system monitoring and protection, as well as logic control functions. In all SBLOCA tests, data were recorded at a frequency of 1 Hz.

4. ACC nitrogen injection comparative tests

Two comparative test groups were conducted in the ACME test facility, as shown in Table 4. The first was the 2-inch cold leg break, which was in the CAP03 and CAP12 tests, and the second was the DEDVI break, which was in the CAP01 and CAP23 tests. The two break scenarios are essential and considered as the reference tests in the previous AP600/1000 test programs. There was only one difference between the two comparative tests. It concerns the configuration of the isolation condition of the ACC after it was empty. In the CAP03 and CAP01 tests, the ACC isolation valves remained open after the ACC became empty, which faithfully simulated the prototypic situation. By contrast, in the CAP12 and CAP23 tests, the ACC isolation valves were closed immediately once the ACC was empty, which was different from the prototypic situation. Additionally, as shown in Table 4, the single failure condition was incorporated into these SBLOCA tests. The condition was that one ADS-4 valve on the non-PZR (pressurizer) side failed to open.

5. Comparison of experimental data

5.1. *The SBLOCA chronologies*

Prior to conducting the comparative tests, repetitive tests were conducted so as to check on the repeatability of the test facility. As the condition of the ACC N_2 injection was the only difference in the test condition, system responses and thermal hydraulic behaviors prior to the emptying of the ACC were the same. However, there were some minor differences because of the minor differences in the initial and boundary test conditions, e.g., the initial liquid level in the component, and the temperature of the coolant in the CMT, ACC, and IRWST. In this study, the comparison of experimental data

Table 3 – Main instruments in ACME test facility and their respective error.

Tag	Instrumentation	Function	Range	Error of instrument
TE	Thermocouple	Temperatures of fluid, wall and heater rods.	350°C	±1.1°C
PT	Pressure transducer	Static pressures of systems and components	10/2/0.5 MPa	0.12/0.075/0.075%
LDP/DP	Differential pressure transducer	Pressure drop and water levels	500/100/10 kPa	0.065%
FE	Bar flow meter	Liquid flow rates	220 m^3/h	1–5% R
FV	Vortex flow meter	Vapor flow rates	5,500 m^3/h	1% R
LM	Guided wave radar	Mixture levels of core and IRWST	1,700 mm	±3 mm
PM	Power meter	Core decay power	4,000 A/500 V	0.5/0.7%
DAS	Data acquisition system	Data acquisition (1–20 Hz)	4–20 mA	0.5%

ACME, advanced core-cooling mechanism experiment; IRWST, in-containment refueling water storage tank.

Table 4 – ACME comparative tests of the ACC N_2 injection effect.

Test no.	Break	Location	Component failure configuration	ACC nitrogen
CAP03	2-inch	3# CL	ADS-4-1A valve on non-PZR	Injected
CAP12	2-inch	3# CL	ADS-4-1A valve on non-PZR	Isolated
CAP01	DEDVI	1# DVI	ADS-4-1A valve on non-PZR	Injected
CAP23	DEDVI	1# DVI	ADS-4-1A valve on non-PZR	Isolated

ACC, accumulator; ACME, advanced core-cooling mechanism experiment; CL, cold leg; DEDVI, double-ended DVI; DVI, direct vessel injection; PZR, pressurizer.

Please cite this article in press as: L. Yuquan et al., Comparative Experiments to Assess the Effects of Accumulator Nitrogen Injection on Passive Core Cooling During Small Break LOCA, Nuclear Engineering and Technology (2016), http://dx.doi.org/10.1016/j.net.2016.06.014

only focused on the transient after the ACC has been emptied. Table 5 summarizes the sequence and timings of the events of selected SBLOCA tests. In the table, the event timings of "ACC emptied" and "IRWST injection" have been derived from the ACC liquid level data and the IRWST injection flow rate data, and the other signals have been recorded by the DCS automatically. For the group with the 2-inch break, the timings of the events prior to the ACC injection were the same as those in CAP03 and CAP12 tests. For the group with the DEDVI break, in the CAP23 test, the actuation of ADS-1 was 8 s later than that in the CAP01 test, which was attributable to the minor differences in the initial and boundary conditions. Moreover, the difference in the recorded ACC empty timings was mainly caused by the measurement errors. In the nitrogen isolation test, the recorded ACC empty timing was actually the same as the time when the ACC isolation valves were programmed to close. In the program, the isolation valve was actuated when the ACC liquid level was at 5 mm. Hence, the recorded ACC empty timing tended to be earlier than the time when the ACC was actually empty. As there were errors in the measurements of the ACC liquid level, especially during its injection process, the recorded ACC empty timings in the CAP03 and CAP01 tests were not exact. By scrutinizing the ACC liquid level and its injection flow rate data, it is estimated that the difference between the recorded and the actual ACC empty timings was ~20 s.

Table 5 – Sequence and timings of events in CAP03/12 and CAP01/23 tests (second).

Event	CAP03	CAP12	CAP01	CAP23
Break	0	0	0	0
PRHR open	0	0	0	0
CMT valve open	0	0	0	0
MS valve shut	0	0	0	0
RCP stop	160	160	50	50
ADS-1 open	675	675	169	177
ADS-2 open	737	738	233	241
ADS-3 open	807	807	302	310
ACC injection	765	765	187	192
ACC emptied	1,204	1,168	512	480
IRWST valve open	1,422	1,402	318	325
ADS-4A open	1,422	1,402	318	325
ADS-4B open	1,457	1,438	352	361
IRWST injection	1,558	1,540	532	497
T-1[a]	657	636	131	133
T-2[b]	218	234	−194	−155
T-3[c]	136	138	214	165
T-4[d]	747	727	149	148

ACC, accumulator; ADS, Automatic Depressurization System; CMT, core makeup tank; IRWST, in-containment refueling water storage tank; MS, main steam; PRHR, passive residue heat removal; RCP, reactor coolant pump.

[a] The transient period between the ACC injection startup and the ADS-4 actuation.

[b] The transient period between the ACC empty and the ADS-4 actuation.

[c] The transient period between the ADS-4 actuation and the onset of IRWST injection.

[d] The transient period between the ADS-1 actuation and the ADS-4 actuation.

In order to compare the chronologies under the opposite N_2 injection condition, the time intervals between the important events were computed, as shown in Table 5. First, the actuation of ADS-4 in the CAP03 test was 20 s later than that in the CAP12 test. As a consequence, the T-1 period in the CAP03 test was longer than that in the CAP12 test. This is an indication that the ACC N_2 injection delays ADS-4 actuation in the 2-inch break test. However, the T-1 periods in the two DEDVI break tests were about the same. This is because ADS-4 was actuated by the CMT on the break side. Furthermore, the T-2 results show that in the 2-inch break test, ADS-4 was actuated after the ACC emptied. However, in the DEDVI break tests, ADS-4 was actuated even before the ACC has emptied. Moreover, similar to the T-1 period, the T-2 period in the CAP03 test was also longer than that in the CAP12 test.

In the CAP03 and CAP12 tests, the T-3 periods were about the same. However, the T-3 period in the CAP01 test was longer than that in the CAP23 test. These results show that N_2 injection had an insignificant effect on the IRWST injection startup in the tests with the 2-inch break, but it delayed the startup in the tests with the DEDVI break. The T-4 period in the CAP03 test was 20 s longer than that in the CAP12 test. This was due to the 20-second late actuation of ADS-4 in the CAP03 test. However, for the tests with the DEDVI break, the T-4 periods are about the same.

In order to explain the differences in the chronologies between the tests, the experimental data of the system responses and core safety are further compared in Sections 5.2 and 5.3.

5.2. *Comparison of CAP03 and CAP12 tests*

The arrow in the experimental data plot indicates the start time of a specific event. As shown in Fig. 4, at the break time, the "S" signal was triggered, and the SG steam line was isolated. The CMT and PRHR isolation valves were then opened, and the reactor coolant pump (RCP) entered into the "coast down" simulation mode. The primary system pressure began

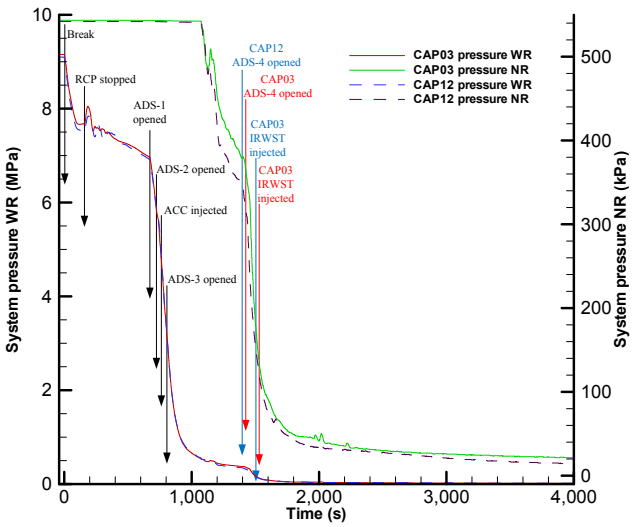

Fig. 4 – History of system pressure and events in CAP03 and CAP12 tests.

Please cite this article in press as: L. Yuquan et al., Comparative Experiments to Assess the Effects of Accumulator Nitrogen Injection on Passive Core Cooling During Small Break LOCA, Nuclear Engineering and Technology (2016), http://dx.doi.org/10.1016/j.net.2016.06.014

to fall when the break opened. When the RCPs stopped, the system pressure rose a little because the system circulation flow slowed down. When the system pressure reached saturation pressure, the CMT started to drain. When the CMT level reached the "Low" level, the ADS-1 valves were opened, and ADS-2 and ADS-3 were subsequently actuated in sequence. Through the ADS-1-3 vent, the system was depressurized very quickly. After the opening of the ADS-2 valve and prior to ADS-3 actuation, the system pressure had already fallen below the ACC N_2 pressure, and the ACC injection started and inhibited the CMT injection. After the ACC became empty, the drainage of the CMT restarted, and then its liquid level dropped to the "Low–Low" level. When the liquid reached this level, ADS-4 opened, which resulted in a fast depressurization of the system. The ADS-4 valves had been set to be opened in sequence according to the control logic, and the "ADS-4 opened" arrow in Fig. 4 marks the time when the ADS-4 valve first opened. When the system was fully depressurized, the IRWST gravity injection started.

The system pressure was recorded with the wide pressure range (10 MPa) and the narrow pressure range (500 kPa), as shown in Fig. 4. The system transient pressure and the event timings between the two tests were practically the same before the ACC was empty. The opening time of ADS-4 in the CAP12 test was 20 s earlier than that in the CAP03 test. Additionally, the startup time of IRWST injection in the CAP12 test was 18 s earlier than that in the CAP03 test. From 1,100 s to 1,450 s, the system pressure in the CAP03 test was slightly higher than that in the CAP12 test. This was the period during which the ACC nitrogen was injected. So, the results show that N_2 injection can cause the system depressurization to slow down. However, once ADS-4 was actuated, the system transient pressures in the two tests were about the same. Additionally, during long-term cooling, the pressure difference between the two tests was too small to be noticed.

As shown in Fig. 5, when the ACC injection started at 765 s, the ACC flow rate increased sharply, and the CMT injection was inhibited. Before the ACC became empty, the flow rates of CMT and ACC in the two tests were practically the same. After the ACC became empty, the CMT injection flow rate in the CAP12 test became more steady and higher than that in the CAP03 test. Furthermore, in the CAP03 test, there were oscillations in the CMT injection flow rate because the ACC nitrogen injection was suppressing the drainage of the CMT intermittently. During this period, in the CAP03 test, N_2 was injected into the system when the pressure difference between the ACC N_2 and the system was greater than the opening resistance of the check valve on the ACC injection line. As a consequence, ADS-4 was opened earlier in the CAP12 test than in the CAP03 test, because of the higher CMT injection flow rate. Additionally, the lower CMT injection flow rate in the CAP03 test led to a higher vapor generation rate when compared to the CAP12 test. This resulted in the slightly higher system pressure in the CAP03 test during the transient between the emptying of the ACC and the ADS-4 actuation. When ADS-4 was opened, the CMT injection flow rate dropped sharply in the CAP03 test because ADS-4 depressurization enhanced ACC N_2 injection as shown in Fig. 5, which, in turn, suppressed the CMT injection. However, in the CAP12 test, the CMT injection rate was basically unaffected after the ADS-4 actuation. This is because the ACC N_2 was isolated from the common DVI line. As ADS-4 was opened earlier in the CAP12 test compared to that in the CAP03 test, the startup of the IRWST injection was also earlier, but the difference in the IRWST injection flow rate between the CAP03 and CAP12 tests was insignificant.

The mixture level, or the so-called "swell level," is caused by steam formation under the two-phase mixture surface because of boiling and flashing during the SBLOCA transient [19], which can be expressed as:

$$H_{\mathrm{mix}} = \frac{H_{\mathrm{collapsed}}}{1 - \langle \alpha_c \rangle}, \tag{1}$$

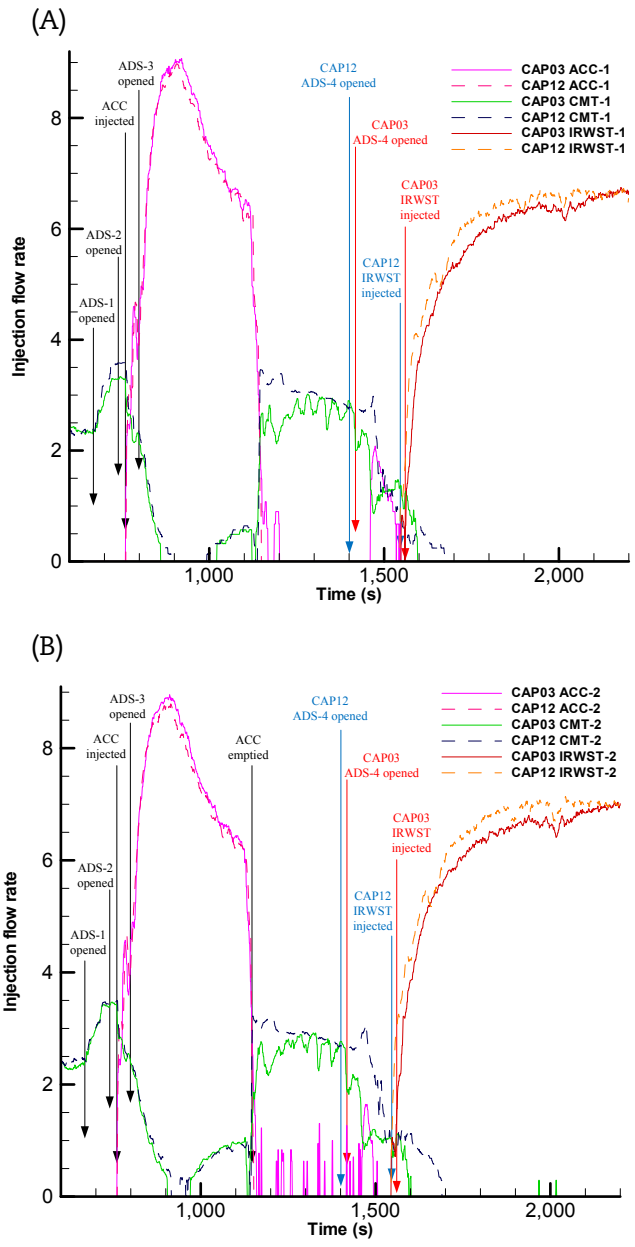

Fig. 5 – CMT, ACC and IRWST injection flow rates in CAP03 and CAP12 tests. (A) DVI-1. (B) DVI-2. ACC, accumulator; CMT, core makeup tank; IRWST, in-containment refueling water storage tank.

Please cite this article in press as: L. Yuquan et al., Comparative Experiments to Assess the Effects of Accumulator Nitrogen Injection on Passive Core Cooling During Small Break LOCA, Nuclear Engineering and Technology (2016), http://dx.doi.org/10.1016/j.net.2016.06.014

where H_{mix} is the mixture level and $H_{collapsed}$ is the collapsed level. $\langle \alpha_c \rangle$ is the average core void fraction. In the ACME test facility, the core collapsed level is measured with a DP transducer. Hence, it is necessary to use a compensation approach to correct the directly measured data so as to accurately obtain the actual water level. The compensation approach can be expressed as:

$$H_{collapsed} = H_{DP}\frac{\rho_{ref}}{\rho_{core}}, \quad (2)$$

where ρ_{ref} is the water density in the DP reference line and ρ_{core} is the fluid density in the core. Therefore, to carry out the compensation according to Eq. (2), it is necessary to find out the liquid density in the core, which varies with temperature and pressure. The core liquid density can be determined from the temperature data measured by the core multipoint TC rod (see Fig. 6) and the system pressure data.

Fig. 7 shows the core mixture and the collapsed levels in the CAP03 and CAP12 tests. The mixture level curves from the two tests are practically overlapping, and the difference in the core collapsed levels between the two tests is insignificant.

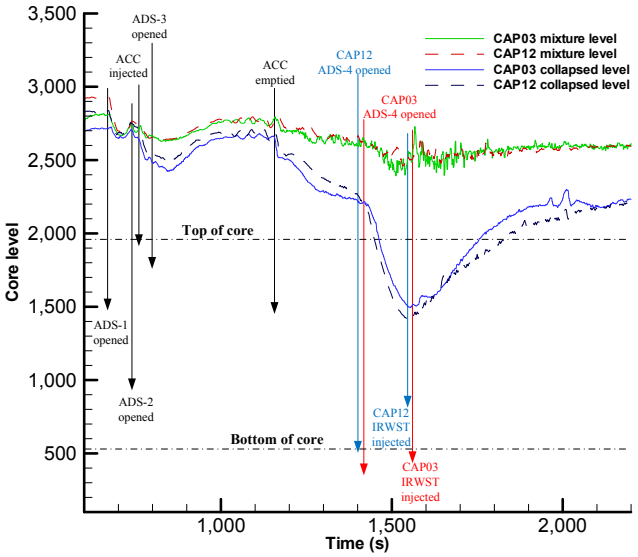

Fig. 7 – Core mixture and collapsed levels in CAP03 and CAP12 tests.

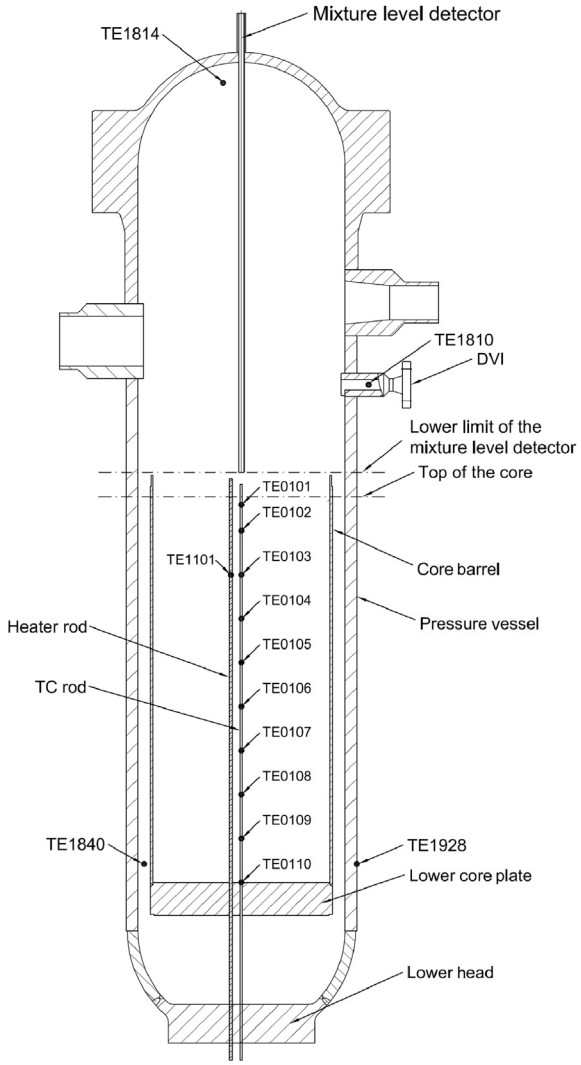

Fig. 6 – The related instruments in RPV. RPV, reactor pressure vessel.

When ADS-1-3 was opened, the core collapsed and the mixture levels dropped, because of the system flashing caused by the fast depressurization. After ADS-2 was opened, the ACC started to rapidly inject its coolant into the system, and as a consequence, the core level increased. When the ACC was nearly empty, the core level began to fall again, and the actuation of ADS-4 caused the core level to fall even faster. During ADS-4 depressurization, the core level kept falling as the entrainment and flashing continued [26]. Prior to the onset of IRWST injection, the core inventory reached the minimum level [5,9–11,13]. In the CAP12 test, the time when the core collapsed level started to rise from its lowest level was slightly earlier than that in the CAP03 test, because of the slightly earlier startup of the IRWST injection. However, the minimum core levels of the two tests were practically the same. Moreover, the core collapsed level rising processes in the two tests were also practically the same. However, the collapsed level in the CAP12 test was slightly lower than that in the CAP03 test. This is because of the slightly higher IRWST water temperature in the CAP12 test as compared to that in the CAP03 test. The higher water temperature corresponds to the season in which the CAP12 test was conducted in summer, and the CAP03 test was conducted in winter. Finally, the comparison results on the core mixture and collapsed levels show that the N_2 injection effect on core level responses is insignificant.

The related instruments in the RPV used for this study are shown in Fig. 6. For the designed cosine axial power distribution, the temperature of the rod is highest near the top of the heated section. This is where the TC had been installed adjacent to the rod clad inner surface, and the peak cladding temperature (PCT) data have been collected. Owing to the constraints in the RPV design, as shown in Fig. 6, the lower limit of the mixture level detector (guided wave radar) was unable to reach the top of the heater rod. As such, the measured core mixture level is not able to show that the core was uncovered.

Please cite this article in press as: L. Yuquan et al., Comparative Experiments to Assess the Effects of Accumulator Nitrogen Injection on Passive Core Cooling During Small Break LOCA, Nuclear Engineering and Technology (2016), http://dx.doi.org/10.1016/j.net.2016.06.014

Fig. 8 shows the PCT (monitored by the TE1101 as shown in Fig. 6) and the core fluid temperature data in CAP03 and CAP12 tests. Before the ACC became empty, the PCT and core fluid temperature curves of the two tests were practically overlapping. After the actuation of ADS-1, both the PCT and the core fluid temperature fell because of the system depressurization. After the ACC became empty, there were oscillations in the middle core fluid temperature in the CAP03 test that were consistent with the CMT injection flow oscillations. This is because the ACC N_2 injection suppressed the CMT injection intermittently. But it should be noted that the oscillations of the injection flow rate had an insignificant impact on the fluid temperatures at the core entrance and the core exit. This was because the fluid was subcooled at the core entrance and became a two-phase saturated mixture at the core exit. However, the fluid temperature at the middle core elevation in the CAP12 test remained fairly constant and was lower than that in the CAP03 test. This was because the CMT injection flow rate remained steady and was higher than that in the CAP03 test, as shown in Fig. 5. Although the core fluid temperature showed several differences, the PCT data from the two tests were the same. This is an indication that core boiling is an extremely effective heat transfer mechanism [6] such that the limited difference in the injection flow rates has little effect on the PCT as long as the core is sufficiently surrounded by fluid. Therefore, the N_2 injection does not affect the PCT.

The N_2 injected from the ACC was discharged through the break, and the ADS-1-3 and ADS-4 venting paths. As shown in Fig. 9, the ADS-1-3 vapor flow rate and the PZR level response during the transient between the two tests are similar. The ADS-1-3 actuation caused the PZR to refill. After the actuation of ADS-4, the PZR started to drain, and the ADS-1-3 vapor flow rate decreased significantly to a low level. The N_2 injection did not lead to a noticeable increase in the ADS-1-3 vapor flow rate, nor did it affect the PZR level response.

As shown in Fig. 10, once the valve was opened, the ADS-4 vapor flow rate immediately reached a peak. The flow rate in

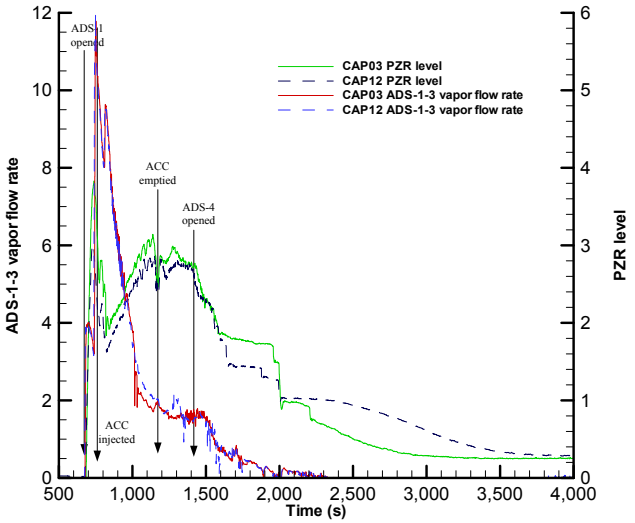

Fig. 9 – PZR water level and ADS-1-3 vapor flow rate in CAP03 and CAP12 tests. PZR, pressurizer.

ADS-4-1 was lower than that in ADS-4-2 because in the simulation, one ADS-4-1 valve failed to open. Additionally, prior to the IRWST injection, the ADS-4-1 flow rate in the CAP12 test was lower than that in the CAP03 test. This was because in the CAP12 test, there was a higher CMT injection flow rate and hence a lower vapor generation rate as compared to that in the CAP03 test. During long-term cooling, the ADS-4 vapor flow rates of the two tests were practically the same. Hence, N_2 injection did not increase the ADS-4 gas-phase discharge flow rate.

The ACC outlet temperature data in the CAP03 and CAP12 tests are shown in Fig. 11. The initial ACC coolant temperature in the CAP03 test was slightly lower than that in the CAP12 test. This was because the tests were conducted in different seasons. In the CAP03 test, there were sharp decreases in the ACC outlet temperature after the ACC became empty. This

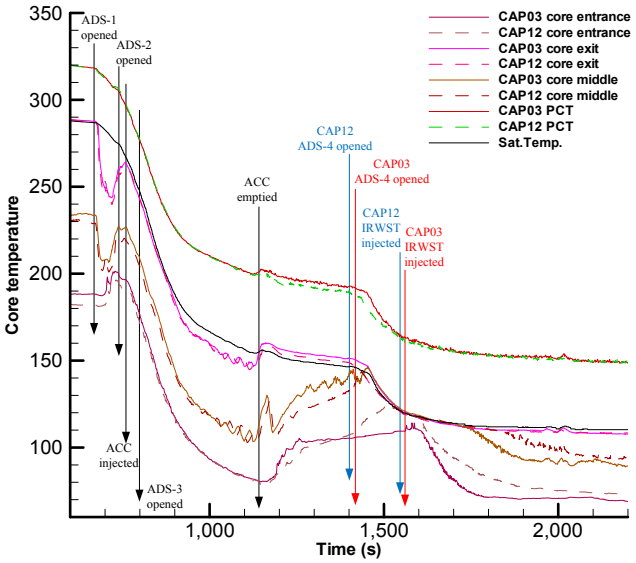

Fig. 8 – PCT and core fluid temperature in CAP03 and CAP12 tests. PCT, peak cladding temperature.

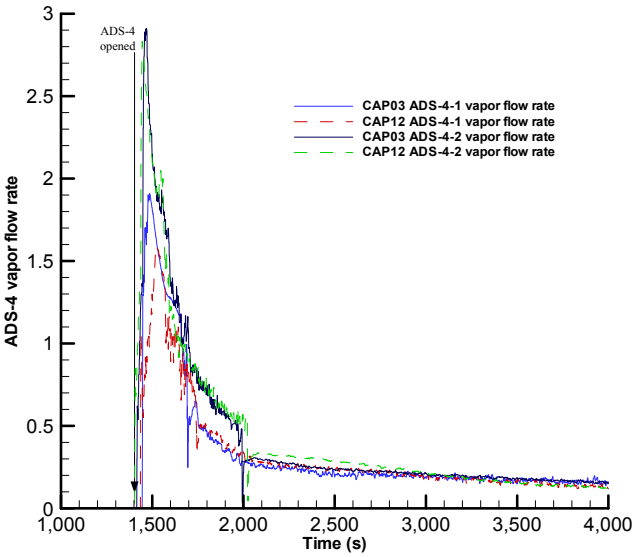

Fig. 10 – ADS-4 vapor flow rate in CAP03 and CAP12 tests. ADS, automatic depressurization system.

Please cite this article in press as: L. Yuquan et al., Comparative Experiments to Assess the Effects of Accumulator Nitrogen Injection on Passive Core Cooling During Small Break LOCA, Nuclear Engineering and Technology (2016), http://dx.doi.org/10.1016/j.net.2016.06.014

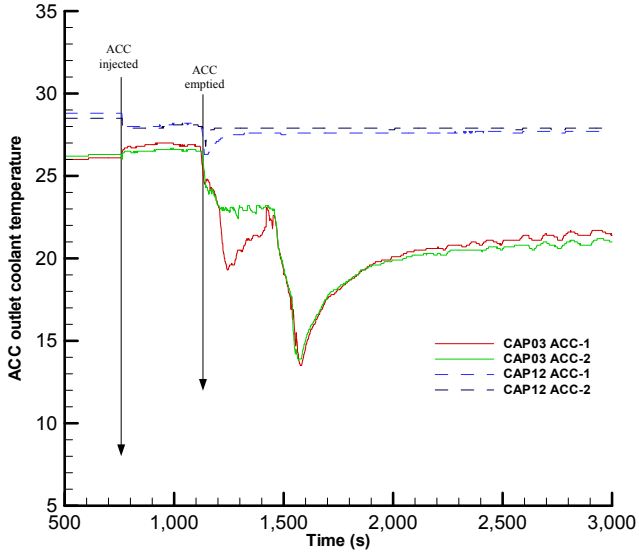

Fig. 11 – ACC outlet temperature data in CAP03 and CAP12 tests. ACC, accumulator.

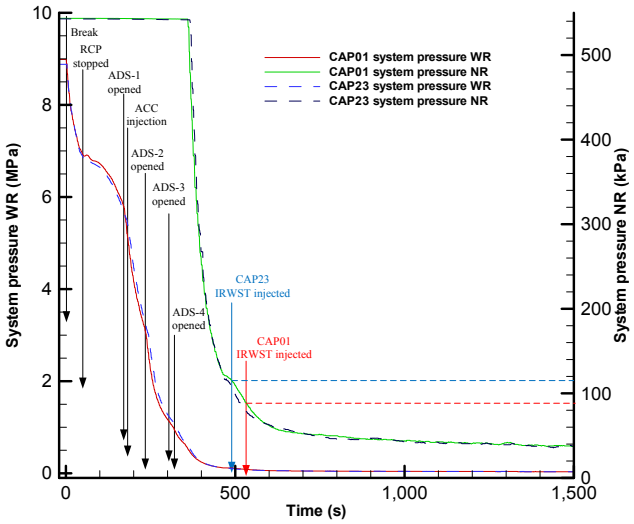

Fig. 12 – History of system pressures and events in CAP01 and CAP23 tests.

was because N_2 was injected by the gas expansion. And then it slowly increased to the environment temperature as the N_2 expansion strength declined with time. However, in the CAP12 test, owing to the isolation of N_2 in the ACC, N_2 was unable to expand. As a consequence, the ACC outlet temperature stayed higher and more stable than that in the CAP03 test. So the N_2 expansion also led the injected gas temperature to decrease, but the calories absorbed by N_2 has been estimated in Section 6.2.

5.3. *Comparison of CAP01 and CAP23 tests*

CAP01 and CAP23 are the DEDVI break tests, in which half of the PXS coolant bypasses the core through the break DVI line. As shown in Fig. 12, as compared to the 2-inch break tests (Fig. 4), the system depressurized much faster and the transient was much shorter for the tests with the DEDVI break. This was because after the break, the CMT on the break side became empty immediately, and ADS-1-3 and ADS-4 were actuated within a short time. As a consequence, IRWST injection started less than 500 s after the break.

In the CAP23 test, the actuations of the ADS-1-3 and ADS-4 valves were 7–8 s later than those in the CAP01 test. This small difference in the timings did not affect the test repeatability, and the pressure curves of the two tests nearly overlapped. Even though the ADS actuations were slightly later in the CAP23 test, the startup of the IRWST injection was 35 s earlier than that in CAP23. As a consequence, after the startup of the IRWST injection in the CAP23 test, the system pressure in the CAP23 test was slightly lower than that in the CAP01 test until the startup of the IRWST injection in the CAP01 test. During the long-term IRWST injection core cooling, the system pressures of the two tests were practically the same. Therefore, similar to the 2-inch break comparison results, the effect of N_2 injection on system pressure response is insignificant.

For the tests with the DEDVI break, only the injection flow rate in the intact DVI line in the two tests were compared. After the ACC became empty, the difference in the CMT injection flow rates between the CAP01 and CAP23 tests was significantly larger than that between the CAP03 and CAP12 tests, as shown in Fig. 13. In the CAP23 test, once the ACC was isolated, the CMT injection returned to a high flow rate, and the IRWST injection started quickly. The CMT injection flow rate decreased as its water head decreased with time. However, in the CAP01 test, when the ACC was empty, the drainage of the CMT was strongly affected by the ACC N_2 injection. As a consequence, the CMT injection flow rate in the CAP01 test was significantly lower than that in the CAP23 test. As N_2 was continuously injected into the system, the ACC N_2 injection suppression

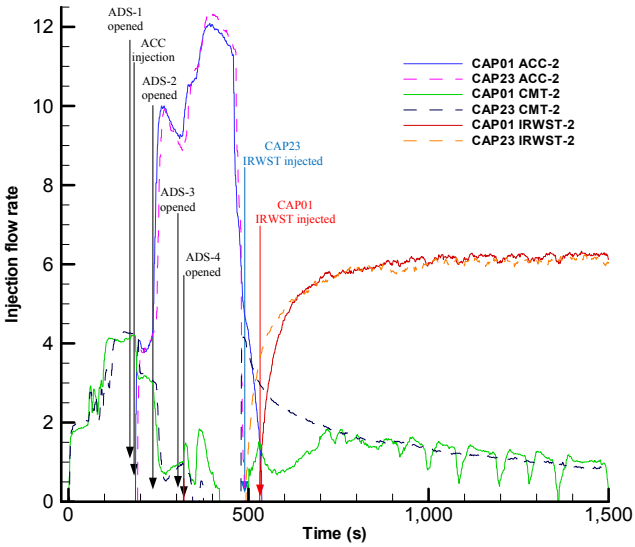

Fig. 13 – CMT-2, ACC-2 and IRWST-2 injection flow rates in CAP01 and CAP23 test. ACC, accumulator; CMT, core makeup tank; IRWST, in-containment refueling water storage tank.

Please cite this article in press as: L. Yuquan et al., Comparative Experiments to Assess the Effects of Accumulator Nitrogen Injection on Passive Core Cooling During Small Break LOCA, Nuclear Engineering and Technology (2016), http://dx.doi.org/10.1016/j.net.2016.06.014

effect became weaker. After nearly 700 s, the CMT injection flow rate in the CAP01 test eventually increased to the same rate as in the CAP23 test. However, there are several sudden decreases in the CMT injection flow rate in the CAP01 test after 700 s. This was because the intermittent N_2 injection occurred when the pressure difference between the ACC N_2 and the system was greater than the opening resistance of the check valve on the ACC injection line.

In addition to the significant difference in the CMT injection flow rate, the startup of the IRWST injection in the CAP01 test was 35 s later than that in the CAP23 test. The low CMT injection flow rate and the later IRWST injection startup resulted in an insufficient injection to the core during the transient between the ACC empty and the IRWST injection startup. Therefore, as compared to the safety injection with the 2-inch break, the ACC N_2 injection effects on the drainage of the CMT and the startup of the IRWST injection were more negative than those on the safety injection with the DEDVI break.

Compared to the system with the 2-inch break, the core mixture and collapsed levels were significantly lower in the system with the DEDVI break. This was because half of the PXS injection failed. Compared to the system with the 2-inch break, the differences in the core level responses became more significant. The low CMT injection flow rate and the later IRWST injection startup resulted in a decrease in the minimum core level in the CAP01 test, as shown in Fig. 14. After the actuation of ADS-4, the injection flow rate in CAP01 was lower than that in CAP23, which led a mixture level swell due to core boiling [19] in CAP01 is stronger than that in CAP23. Because the detector (guided wave radar) became sensitive when the mixture level was getting close to its lower limit, the mixture level data showed drastic oscillations. Moreover, in the CAP01 test, before the IRWST injection reached the maximum flow rate, the core mixture level fell below even the lower limit of the mixture level detector. Therefore, the comparison result confirms that ACC N_2 injection has a significant negative impact on the core minimum level in the system with the DEDVI break. However, during long-term core cooling, the core levels of the two tests were practically the same.

As shown in Fig. 15, the PCT and the fluid temperatures at the top and middle elevations of the core in the two tests were practically the same. Furthermore, there was a difference in fluid temperatures at the core entrance only between 500 s and 900 s. After the ADS-4 actuation, the core fluid became largely saturated because of the fast depressurization of the system. However, as the ACC injection was enhanced by the ADS-4 depressurization, the core entrance fluid returned to subcooled temperature until the ACC was emptied. After the ACC became empty at ~500 s, similar to the comparison results on the core level responses, there was a difference in the core entrance temperatures in the two tests until 800 s. In the CAP23 test, because of the isolation of the ACC N_2, the CMT injection was immediately restored to a high flow rate, and the IRWST injection started in time, which provided the necessary injection to the core. As a consequence, the core entrance fluid remained subcooled in the CAP23 test. However, it quickly increased to the saturation temperature in the CAP01 test because of insufficient coolant injection. Once the IRWST injection stabilized in the CAP01 test, the core entrance temperature decreased gradually to the same temperature as in the CAP23 test. Additionally, the core middle and exit remained at the saturation temperature even though the core entrance temperatures in the two tests were significantly different. Therefore, the N_2 injection affected the core entrance temperature, but does not affect the core two-phase region temperature and the PCT.

As shown in Fig. 16, similar to the system with the 2-inch break, the PZR was refilled during ADS-1-3 depressurization, and started to drain when ADS-4 was opened. Because of the small injection flow rate in the system with the DEDVI break, the vapor generation rate remained high, which reduced the PZR drainage rate. After the ACC became empty, the ADS-1-3 vapor flow rate curves of the CAP01 and CAP23 tests practically overlapped. Therefore, similar to the 2-inch break comparison

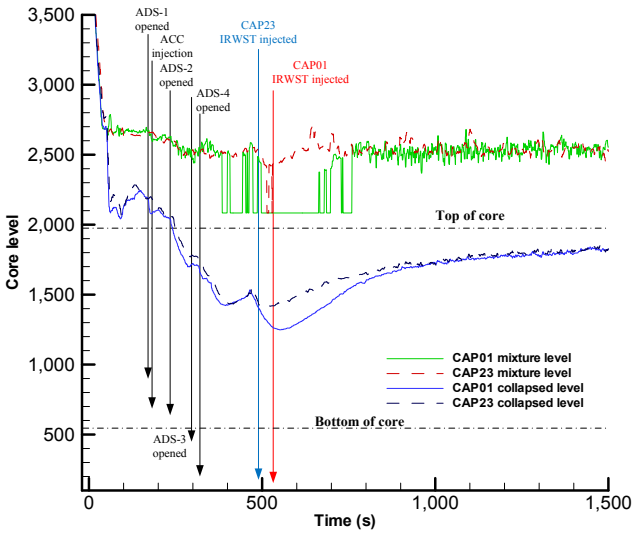

Fig. 14 – Core mixture and collapsed levels in CAP01 and CAP23 test.

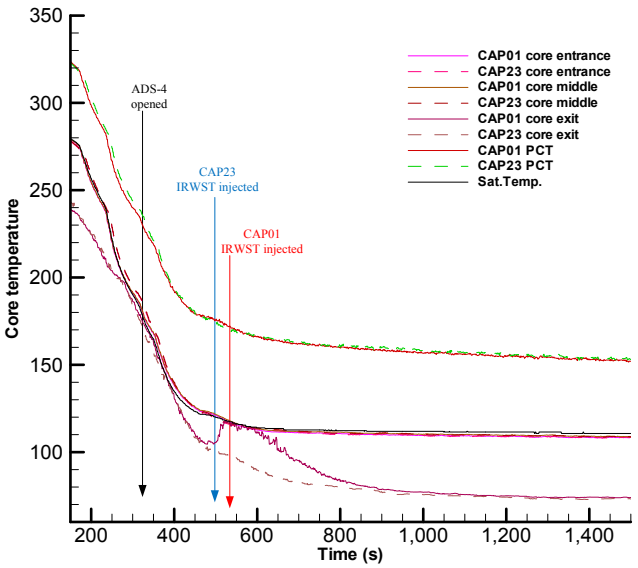

Fig. 15 – PCT and core fluid temperature in CAP01 and CAP23 test. PCT, peak cladding temperature.

Please cite this article in press as: L. Yuquan et al., Comparative Experiments to Assess the Effects of Accumulator Nitrogen Injection on Passive Core Cooling During Small Break LOCA, Nuclear Engineering and Technology (2016), http://dx.doi.org/10.1016/j.net.2016.06.014

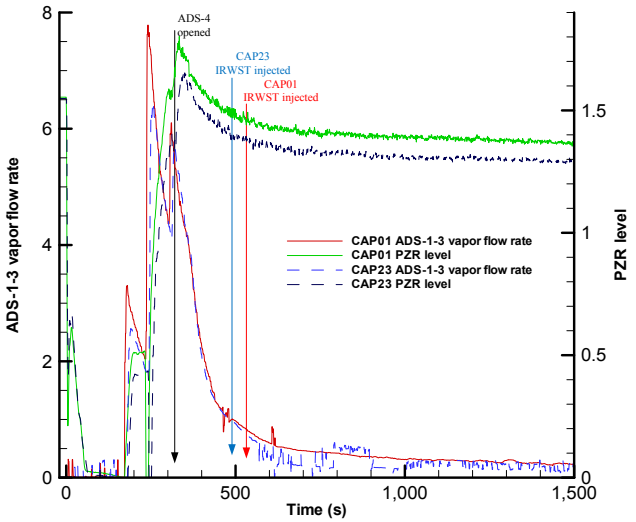

Fig. 16 – PZR water level and ADS-1-3 vapor flow rate in CAP01 and CAP23 tests. ADS, automatic depressurization system; PZR, pressurizer.

results, there is no noticeable ACC N_2 injection effects on the PZR level response and the ADS-1-3 vapor flow rate.

As shown in Fig. 17, after the ACC became empty at ~500 s, the vapor flow rate in ADS-4-2 in the CAP01 test was higher than that in the CAP23 test. This was because the vapor generation rate in the CAP01 test was higher than that in the CAP23 test. Also, in the CAP01 test, both the CMT injection and startup of the IRWST injection were suppressed by the ACC N_2 injection. Moreover, the resistance of ADS-4-2 was smaller than that of ADS-4-1. This was because one ADS-4-1 valve failed to open. The difference in the ADS-4-2 discharge flow rates was more noticeable that that in the ADS-4-1. However, during the long-term IRWST injection, the ADS-4 vapor flow rate of the two tests remained unaffected, and this observation was similar to the 2-inch break test results.

Similar to the 2-inch break test comparison results, as shown in Fig. 18, the ACC outlet temperature in the CAP23 test remained higher and more stable than that in the CAP01 test. Furthermore, when N_2 injection started in the CAP01 test, there was a sharp drop in the ACC outlet temperature, and the temperature increased slowly with time because of the decline in intensity of the N_2 expansion. During the long-term cooling process in the CAP01 test, there were small oscillations in the ACC outlet temperature, which were caused by the intermittent N_2 injection during ACC N_2 expansion.

6. Discussion

6.1. The break condition

The results of the two comparative test groups show that N_2 injection suppresses the drainage of the CMT and delays the startup of the IRWST injection. However, in the 2-inch break case, the system responses and the core safety are basically unaffected. But in the DEDVI case, the N_2 injection significantly decreases the CMT injection flow rate and delays the IRWST injection startup. As a consequence, the minimum core level decreases, resulting in a much longer time for the core level to rise from its minimum level to the long-term cooling level. Therefore, the effects of N_2 injection on system responses and core safety depend on the type of break.

In the 2-inch break tests, as shown in Table 5, the ACC started to inject soon after the actuation of ADS-2, and became empty prior to the actuation of ADS-4. Because the ACC injection can inhibit the drainage of the CMT and ADS-4 was actuated only when the liquid level in the CMT reached the "Low–Low" set point level, the ACC was already emptying and could inject a portion of the ACC N_2 into the system prior to the actuation of ADS-4. The amount of N_2 injected into the system depends on the system depressurization and the CMT inventory above the "Low–Low" level by the time the ACC is

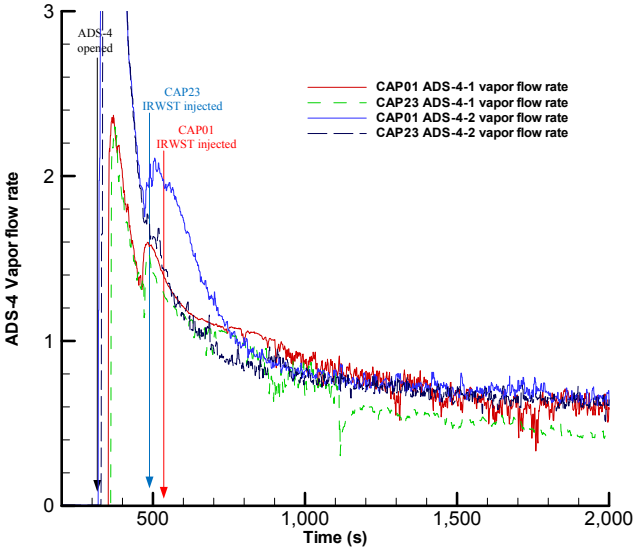

Fig. 17 – ADS-4 vapor flow rate in CAP01 and CAP23 tests. ADS, automatic depressurization system.

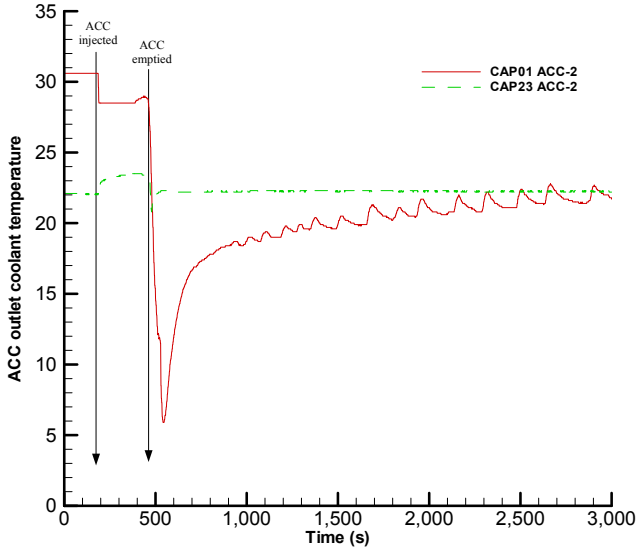

Fig. 18 – ACC-2 outlet temperature data in CAP01 and CAP23 tests. ACC, accumulator.

Please cite this article in press as: L. Yuquan et al., Comparative Experiments to Assess the Effects of Accumulator Nitrogen Injection on Passive Core Cooling During Small Break LOCA, Nuclear Engineering and Technology (2016), http://dx.doi.org/10.1016/j.net.2016.06.014

empty. Because of the partial release of the ACC N_2, N_2 expansion and its injection suppression effect becomes smaller during ADS-4 depressurization, and hence its effects on system responses and core safety are also lessened.

However, in the DEDVI break tests, as the ADS-4 was actuated by the CMT on the break side, the functional ACC was empty even after the actuation of ADS-4. As such, the expansion and injection of the ACC N_2 only happened after the actuation of ADS-4. In fact, the fast depressurization of the system by ADS-4 even enhanced the N_2 expansion and injection. As a consequence, there was a large decrease in CMT injection flow, which slowed down the system depressurization because of the increase in the vapor generation rate, as shown in Figs. 12 and 17. More importantly, as shown in Fig. 12, the IRWST injection started in the CAP23 test when the system pressure dropped to nearly 115 kPa. By contrast, in the CAP01 test, the IRWST injection only started when the system dropped to below 90 kPa. The water heads of the IRWST of the two tests were the same. So, the comparison on the system pressure on the IRWST startup time shows that the startup of the IRWST injection is also affected by N_2 injection.

Therefore, the event sequence between the ACC being empty and the ADS-4 actuation largely controls the effects of the N_2 injection. In the case in which the ACC empties after ADS-4 actuation, N_2 injection plays an important role in suppressing the CMT injection and delaying the IRWST injection startup, which results in a large drop in the minimum core level.

However, for most SBLOCA cases like the small break on the main pipe, as the drainage of the CMT is suppressed by the ACC injection until the ACC is empty, the ACC N_2 is already partially released prior to ADS-4 actuation. In that case, the effect of N_2 injection on the system is lessened to the extent that it becomes unimportant, and the minimum core level is likely to remain unaffected.

6.2. N_2 injection amount evaluation

In the SBLOCA cases, once ADS-1-3 and ADS-4 are opened, they become the system's main venting path. Usually, the ACC empties after the actuation of ADS-1-3. So, the ACC N_2 flows out of the system mainly through the ADS venting paths. However, considering the measurement errors, the comparison of experimental results in this study is insufficient to give any direct evidence that N_2 injection causes the increases in the vapor flow rates of ADS-1-3 and ADS-4. Moreover, the system pressures in the comparison tests also remain mostly unaffected. During the transient from the time when the ACC is empty to the startup of the IRWST injection, the system pressure in the N_2 injection test is slightly higher than that in the N_2 isolation test. This is mainly attributable to the suppression of the CMT injection, which causes an increase in core vapor generation. This suggests that N_2 injection did not directly lead to the increase in system pressure. Therefore, according to this suggestion, the amount of ACC N_2 injected into the system is insignificant compared to the vapor generation in the system. To be able to justify the previous statement, the amount of N_2 gas injected into the system with its possible effects need to be evaluated, as follows.

The amount of nitrogen gas precharged in the ACC can be determined by:

$$P_{\text{initial}} V_{\text{initial}} = m_{N_2,\text{ACC}} R_g T \tag{3}$$

The nitrogen expansion injection process can be approximated as a reversible adiabatic expansion of a perfect gas. So, the relationship between the pressure and volume is:

$$\frac{P_{\text{final}}}{P_{\text{initial}}} = \left(\frac{V_{\text{initial}}}{V_{\text{expansion}}}\right)^{\kappa}, \tag{4}$$

where P_{initial} and P_{final} are the ACC initial charge pressure and the fully depressurized system pressure, respectively. V_{initial} and $V_{\text{expansion}}$ are the initial volume of N_2 in the ACC and the fully expanded volume at P_{final}, respectively. κ is the ratio of specific heats, and for N_2, $\kappa = 1.4$. After the gas expansion, most of the ACC N_2 is injected into the system, but a fraction of N_2 remains in the ACC. So, the mass of injected N_2 can be determined from:

$$m_{N_2,inj} = \frac{V_{\text{expansion}} - V_{\text{ACC}}}{V_{\text{expansion}}} m_{N_2,\text{ACC}} \tag{5}$$

In addition, because of the expansion of ACC N_2 in the gas space, the gas is injected into the system. Furthermore, during the injection and system depressurization, the N_2 that has dissolved in the ACC coolant is also released into the system. The mass of N_2 that dissolves in the ACC coolant can be determined using Henry's law, which is:

$$H^{cp} = c_a / P, \tag{6}$$

where H^{cp} is Henry's constant [mol/(m^3 Pa)], c_a is the concentration of a species in the aqueous phase (mol/m^3), and P is the partial pressure of that species in the gas phase under the equilibrium condition. In this study, the initial nitrogen gas pressure $P_{\text{initial}} = 4.93$ MPa, and the liquid temperature is about 40°C. The corresponding Henry's constant [27] is 5.29×10^6 mol/(m^3 Pa). The amount of N_2, which dissolves in the ACC coolant, can be determined by:

$$m_{N_2,\text{dis}} = M_{N_2} H^{cp} P_{\text{initial}} V_{\text{ACC}} (1 - \alpha) \tag{7}$$

In this study, it is assumed that N_2 in the system is heated up to system saturation temperature, and the dissolved N_2 completely comes out of the coolant. As such, the final volume of N_2 in the system can be determined by:

$$V_{N_2,\text{final}} = \frac{(m_{N_2,\text{inj}} + m_{N_2,\text{dis}}) R_g T_{\text{sat}}}{P_{\text{final}}} \tag{8}$$

According to the ideal gas law, the N_2 gas temperature decreases after its expansion, and the injected N_2 temperature can be determined from:

$$\frac{T_{\text{expansion}}}{T_{\text{initial}}} = \left(\frac{P_{\text{final}}}{P_{\text{initial}}}\right)^{\frac{k-1}{k}} \tag{9}$$

The heat absorption by the N_2 gas entering into the system can be determined by:

$$Q_{N_2,\text{sys}} = m_{N_2,\text{inj}} C_P (T_{\text{sat}} - T_{\text{expansion}}) + m_{N_2,\text{dis}} C_P (T_{\text{sat}} - T_{\text{initial}}) \tag{10}$$

The amount of N_2 injected into the system and the amount of heat absorbed in the plants and the ACME test facility are listed in Table 6.

In this study, to directly facilitate the evaluation of the N_2 effect on the system transient, the time in which the vapor

Please cite this article in press as: L. Yuquan et al., Comparative Experiments to Assess the Effects of Accumulator Nitrogen Injection on Passive Core Cooling During Small Break LOCA, Nuclear Engineering and Technology (2016), http://dx.doi.org/10.1016/j.net.2016.06.014

Table 6 – Results of nitrogen injection related calculations for AP600, AP1000, CAP1400 and ACME.

	AP600	AP1000	CAP1400	ACME
Mass of N_2 in each ACC gas space (kg)	454	454	623	6.62
Mass of N_2 dissolved in each ACC liquid (kg)	35	35	49	0.516
Mass of injected and released N_2 in each ACC (kg)	289	289	397	4.22
Final volume of N_2 in system from each ACC (m^3)	291	291	400	4.25
Energy absorbed by N_2 in each ACC (MJ)	72.7	72.7	99.91	1.061
Core decay power (1% nominal power) (MW)	19.33	34	40.4	0.744
Maximum core vapor generation rate (m^3/s)	12.2	21.5	25.6	0.471
Equivalent vaporization period (two ACCs) (s)	47.7	27.1	31.3	18
Equivalent core heating period (two ACCs) (s)	7.5	4.3	4.9	2.85

ACC, accumulator; ACME, advanced core-cooling mechanism experiment.

with the final N_2 volume is generated by the core decay power, is referred to as the equivalent vaporization period, which is:

$$\tau_V = \frac{V_{N_2,final}\rho_{gs}h_{fg}}{\dot{Q}_{core}} \quad (11)$$

Furthermore, the time in which the energy that is equivalent to the heat absorbed by N_2 is generated by the core decay power, is referred to as the equivalent core heating period, which is:

$$\tau_Q = \frac{Q_{N_2,sys}}{\dot{Q}_{core}} \quad (12)$$

In this study, for a conservative evaluation of the effects of N_2 gas, the decay power is assumed to be 1% of the nominal power. This is because the core power is usually higher than the assumed decay power when the ACC is empty in an SBLOCA transient. The results of the calculations are shown in Table 6.

The ACC in the ACME test facility has been designed according to the system scale ratios as shown in Table 2, and it has the same N_2 charge pressure as its prototype. So, N_2 mass, volume, and heat absorption in ACME are all 1/94 scale. Furthermore, as the SBLOCA transient simulated on ACME is accelerated by the time ratio of 1/1.732, the equivalent vaporization period and equivalent core heating period are also all scaled by this ratio. So, the effect of N_2 on system depressurization was evaluated based on the same time scale. In Table 6, it can be seen that the N_2 equivalent vaporization period is much shorter than that of the ADS-4 depressurization transient period (T-3 in Table 5). Furthermore, the equivalent core heating period is even shorter than the equivalent vaporization period. Moreover, the evaluation does not include the vapor generated by the flashing during depressurization, which leads to an overestimation of the N_2 fraction in the system. Therefore, it can be concluded that the N_2 injection amount is not large enough to affect the system pressure, and hence its effect on system depressurization is insignificant. Moreover, the evaluation results of the plants are similar.

7. Conclusion

In this study, comparative tests of the ACC N_2 injection into the core cooling system were conducted in a new integral effect test facility, named ACME. As the experimental data are representative of the system responses and the core safety, the data were analyzed for the assessment of N_2 injection effects on the passive safety core cooling performance during SBLOCA transient and the mechanisms. The conclusions are as follows. (1) The ACC N_2 injection decreases the CMT injection flow rate and delays the IRWST injection. The decrease in CMT injection flow rate has little effect on system depressurization. The effects of N_2 injection on system responses and core safety are related to the type of break. (2) In the case of a main pipe small break, the system responses and the minimum core level remain nearly unaffected. The effect of N_2 injection on the main pipe small break transient is insignificant and does not cause any safety concern. (3) In the DEDVI case, the ACC N_2 injection strongly affects the CMT injection and delays the startup of IRWST drainage. As a consequence, there is a decrease in the minimum core level. The effect of N_2 on DEDVI break transient is significant. However, even though the core inventory is decreased, the PCT remains unaffected. (4) In the main pipe small break case, prior to ADS-4 actuation, N_2 is partially released, which lessens the effects of N_2 injection on system responses and core safety in the ADS-4 depressurization phase. However, in the DEDVI case, the ACC N_2 completely discharges into the system after ADS-4 actuation. This enhances the N_2 injection effect in suppressing the drainage of the CMT and in the startup of IRWST injection. For the case where ACC emptying occurs after ADS-4 actuation, it is important to pay attention to the N_2 injection effect because it decreases the core level. (5) The amount of N_2 injection and the heat absorption are small when compared to the vapor generated in the system and the core decay power heating. For the current passive safety plants design, the injected N_2 pressurization effect is too small to affect the system depressurization directly.

Conflicts of interest

No conflict of interest.

Acknowledgments

The ACME test program was sponsored by the National Science and Technology Major Project of the Chinese Ministry of Science and Technology (Grant No. ZX2011-006-003).

Nomenclature

C_P	Specific heat (kJ/(kg k))
H	Water level (m)
H^{cp}	Henry's constant (mol/(m^3 Pa))
h	Enthalpy (kJ/kg)

Please cite this article in press as: L. Yuquan et al., Comparative Experiments to Assess the Effects of Accumulator Nitrogen Injection on Passive Core Cooling During Small Break LOCA, Nuclear Engineering and Technology (2016), http://dx.doi.org/10.1016/j.net.2016.06.014

H_{fg}	Latent heat (kJ/kg)
m	Mass (kg)
P	Pressure (Pa)
Q	Energy (kJ)
$\dot{Q}_{core}$	Core power (kW)
R_g	Gas constant (J/(kg K))
T	Temperature (K)
V	Volume (m^3)
α	Void fraction, gas fraction
ρ	Density (kg/m^3)
κ	Ratio of specific heats
τ	Equivalent time (seconds)

Subscript

c, core	Core
collapsed	Collapsed level
dis	Dissolved
inj	Injection
gs	Saturate vapor
ls	Saturate liquid
N_2	Nitrogen
mix	Mixture
sys	System

Abbreviation

ACME	Advanced core-cooling mechanism experiment
ACC	Accumulator
ADS	Automatic Depressurization System
BAMS	Break and ADS Measurement System
CL	Cold Leg
CMT	Core Makeup Tank
DCS	Distributed Control System
DEDVI	Double-Ended DVI break
DVI	Direct vessel injection
ECCS	Emergency core cooling system
HL	Hot leg
IRWST	In-containment refueling water storage tank
LOCA	Loss-of-coolant accident
PBL	Pressure balance line
PCT	Peak cladding temperature
PIRT	Phenomena Identification and Ranking Table
PRHR	Passive Residue Heat Removal
PWR	Pressurized water reactor
PXS	Passive core cooling system
PZR	Pressurizer
RCP	Reactor coolant pump
RNS	Normal Residue heat Removal System
RPV	Reactor pressure vessel
SBLOCA	Small break LOCA
SEP	Separator
SG	Steam generator
TC	Thermal couple
TH	Thermal–hydraulic

REFERENCES

[1] Y. Bae, Y.I. Kim, K.K. Kim, Transient performance analysis of pressurized safety injection tank with a partition, Ann. Nucl. Energy 75 (2015) 232–238.

[2] S.N. Tower, T.L. Schulz, R.P. Vijuk, Passive and simplified system features for the advanced Westinghouse 600 MWe PWR, Nucl. Eng. Des. 109 (1988) 147–154.

[3] R.A. Matzie, AP1000 will meet the challenges of near-term deployment, Nucl. Eng. Des. 238 (2008) 1856–1862.

[4] L. Ma, J. Li, S. Ji, H.J. Chang, Turbulent convection experiment at high Rayleigh number to support CAP1400 IVR strategy, Nucl. Eng. Des. 292 (2015) 69–75.

[5] L.M. Shotkin, Y. Kukita, Implications of the ROSA/AP600 high- and intermediate-pressure test results, Nucl. Technol. 119 (1997) 217–234.

[6] J. Reyes, L. Hochreiter, Scaling analysis for the OSU AP600 test facility (APEX), Nucl. Eng. Des. 186 (1998) 53–109.

[7] Yutaka Kukita, Taisuke Yonomoto, Hideaki Asaka, Hideo Nakamura, Hiroshige Kumamaru, Yoshinari Anoda, Timothy J. Boucher, Marcos G. Ortiz, Roy A. Shaw, Richard R. Schultz, ROSA/AP600 testing: facility modifications and initial test results, J. Nucl. Sci. Technol. 33 (1996) 259–265.

[8] R.F. Wright, R. Hundal, L.E. Hochreiter, M.T. Friend, M. Ogrins, Analysis and evaluation of the AP600 SPES-2 integral systems tests, Int. Conf. Nucl. Eng. ASME 2 (1996) 417–425.

[9] M.T. Friend, R.F. Wright, R. Hundal, L.E. Hochreiter, M. Ogrins, Simulated AP600 response to small-break loss-of-coolant-accident and non-loss-of-coolant-accident events: analysis of SPES-2 integral test results, Nucl. Technol. 122 (1998) 19–41.

[10] R.F. Wright, Simulated AP1000 response to design basis small-break LOCA events in APEX-1000 test facility, Nucl. Eng. Technol. 39 (2007) 287–298.

[11] J.N. Reyes Jr., G.T. Groome, A.Y. Lafi, S.C. Franz, C. Rusher, M. Strohecker, D. Wachs, S. Solpo, S. Binney, Final report of NRC AP600 research conducted at Oregon State University, NUREG/CR 6641, U.S. Nuclear Regulatory Commission, Washington, DC 20555-0001, 1999.

[12] W. Wulff, U.S. Rohatgi, System scaling for the Westinghouse AP600 pressurized water reactor and related test facilities, NUREG/CR-5541, BNL-NUREG-52550, U.S. Nuclear Regulatory Commission, Washington, DC 20555-0001, 1998, 1-1 - 9-2.

[13] K.B. Welter, S.M. Bajorek, Reyes Jose Jr., Woods Brain, Groome John, Hopson John, Youny Eric, DeNoma John, Abel Kent, APEX-AP1000 confirmatory testing to support AP1000 Design Certification (Non-Proprietary), U.S. Nuclear Regulatory Commission, Washington, DC 20555-0001, 2005, 1-1 - 7-2, NUREG-1826.

[14] Z.M. Meng, B. Dong, L.S. Wang, X.L. Fu, W.X. Tian, Y.H. Yang, G.H. Su, Experimental research of liquid entrainment through ADS-4 in AP1000, Ann. Nucl. Energy 72 (2014) 428–437.

[15] K.B. Welter, Q. Wu, Y. You, K. Abel, D. McCreary, S.M. Bajorek, J.N. Reyes Jr, Experimental investigation and theoretical modeling of liquid entrainment in a horizontal tee with a vertical-up branch, Int. J. Multiphase Flow 30 (2004) 1451–1483.

[16] Z.M. Meng, X.L. Fu, L. Ding, B. Dong, W.X. Tian, Y.H. Yang, G.H. Su, Experimental and theoretical investigation of liquid entrainment through small-scale ADS-4 in AP1000, Exp. Thermal Fluid Sci. 57 (2014) 177–187.

[17] Z.M. Meng, L.F. Liu, L. Ding, X.L. Fu, W.X. Tian, Y.H. Yang, G.H. Su, Comparative study on effect of air–water and steam–water mediums on liquid entrainment through ADS-4 in AP1000, Exp. Thermal Fluid Sci. 69 (2015) 149–157.

[18] W.W. Wang, G.H. Su, Z.M. Meng, W.X. Tian, S.Z. Qiu, Analyses of liquid entrainment through ADS-4 in AP1000 during a typical small break LOCA transient, Ann. Nucl. Energy 60 (2013) 195–201.

[19] W.W. Wang, G.H. Su, S.Z. Qiu, W.X. Tian, Thermal hydraulic phenomena related to small break LOCAs in AP1000, Prog. Nucl. Energy 53 (2011) 407–419.

Please cite this article in press as: L. Yuquan et al., Comparative Experiments to Assess the Effects of Accumulator Nitrogen Injection on Passive Core Cooling During Small Break LOCA, Nuclear Engineering and Technology (2016), http://dx.doi.org/10.1016/j.net.2016.06.014

[20] H.J. Chang, Y.Q. Li, Q. Wu, Z.S. Ye, L. Chen, A new integral test facility ACME for passive safety PWR, ANS Winter Meeting, 2012, November 11–15, San Diego, CA.
[21] L. Chen, H.J. Chang, Y.Q. Li, Z.S. Ye, B.K. Qin, Analysis on working pressure selection of ACME integral test facility, Atomic Energy Sci. Technol. 45 (2011) 1215–1220.
[22] G.E. Wilson, B.E. Boyack, The role of the PIRT process in experiments, code development and code applications associated with reactor safety analysis, Nucl. Eng. Des. 186 (1998) 23–27.
[23] Zuber Novak, Gary E. Wilson, Ishii Mamoru, Wulff Wolfgang, B.E. Boyack, A.E. Dukler, P. Griffith, J.M. Healzer, R.E. Henry, J.R. Lehner, S. Levy, F.J. Moody, M. Pilch, B.R. Sehgal, B.W. Spencer, T.G. Theofanous, J. Valente, An integrated structure and scaling methodology for severe accident technical issue resolution: development of methodology, Nucl. Eng. Des. 186 (1998) 1–21.
[24] Y.Q. Li, H. Wang, Z.S. Ye, L. Chen, B.K. Qin, ACME test facility scaling analysis report (Ver. A), State Nuclear Power Research and Development Center, Beijing, 2012, p. K001BG0016.
[25] T. Zhang, M.T. Cui, F. Tian, Uncertainty Budget of ACME Instrumentation System (Ver. A), State Nuclear Power Research and Development Center, Beijing, 2014, p. K001BG0052.
[26] D.C. Sun, Y. Xiang, W.X. Tian, J.C. Liu, P. Zhang, S.Z. Qiu, G.H. Su, Experimental investigation of upper plenum entrainment in AP1000, Prog. Nucl. Energy 80 (2015) 80–85.
[27] R. Sander, Compilation of Henry's law constants (version 4.0) for water as solvent, Atmos. Chem. Phys. 15 (2015) 4399–4981.

Please cite this article in press as: L. Yuquan et al., Comparative Experiments to Assess the Effects of Accumulator Nitrogen Injection on Passive Core Cooling During Small Break LOCA, Nuclear Engineering and Technology (2016), http://dx.doi.org/10.1016/j.net.2016.06.014